Taylor & Francis
Taylor & Francis Group

RESEARCH PAPER

Effect of histone demethylase KDM5A on the odontogenic differentiation of human dental pulp cells

Qi-Meng Li[a,#], Jin-Ling Li[a,b,#], Zhi-Hui Feng[a], Huan-Cai Lin[a], and Qiong Xu[a]

[a]Guanghua School of Stomatology, Hospital of Stomatology, Guangdong Provincial Key Laboratory of Stomatology, Sun Yat-Sen University, Guangzhou, Guangdong, P.R. China; [b]Guangdong Provincial Hospital of Chinese Medicine, The Second Affiliated Hospital of Guangzhou University of Chinese Medicine, Guangzhou, Guangdong, P.R. China

ABSTRACT

Human dental pulp cells (hDPCs) possess the capacity to differentiate into odontoblast-like cells in response to exogenous stimuli. Histone methylation is one of the most robust epigenetic marks and is essential for the regulation of multiple cellular processes. Previous studies have shown that histone methyltransferases (HMTs) and histone demethylases (HDMs) are crucial for the osteogenic differentiation of human bone marrow, adipose tissue, and tooth tissue. However, little is known about the role of histone methylation in hDPC differentiation. Here, the expression levels of HMTs and HDMs were profiled in hDPCs undergoing odontogenic induction. Among several differentially expressed enzymes, HDM KDM5A demonstrated significantly enhanced expression during cytodifferentiation. Furthermore, KDM5A expression increased during early passages and in a time-dependent manner during odontogenic induction. Using a shRNA-expressing lentivirus, KDM5A was knocked down in hDPCs. KDM5A depletion resulted in greater alkaline phosphatase activity and more mineral deposition formation. Meanwhile, the expression levels of the odontogenic markers DMP1, DSPP, OSX, and OCN were increased by KDM5A knockdown. As a histone demethylase specific for tri- and dimethylated histone H3 at lysine 4 (H3K4me3/me2), KDM5A deficiency led to a significant increment in total H3K4me3 levels, whereas no significant difference was found for H3K4 me2. H3K4me3 levels on the promoters of the odontogenic markers increased after KDM5A knockdown in hDPCs. These results demonstrated that KDM5A is present in hDPCs and inhibits the odontogenic differentiation potentiality of hDPCs by removing H3K4me3 from specific gene promoters, suggesting that KDM5A-dependent histone demethylation may play an important role in reparative dentinogenesis.
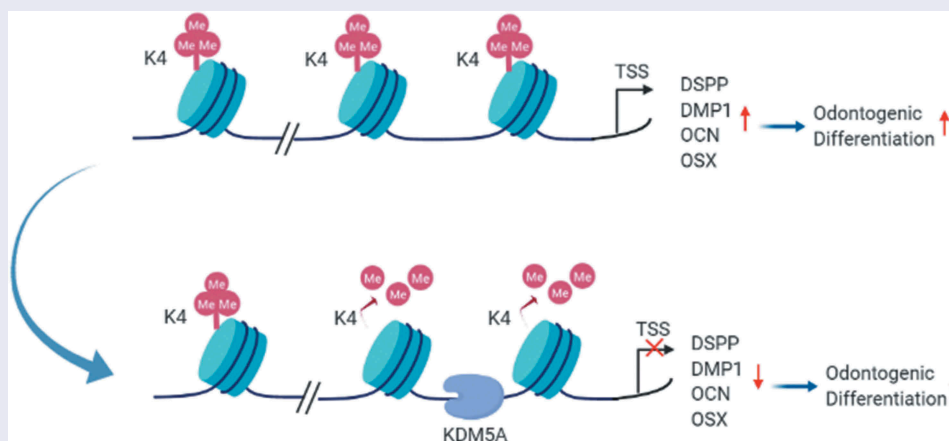
CONTACT Huan-Cai Lin ✉ linhcgz@126.com; Qiong Xu ✉ xqiong@mail.sysu.edu.cn 🔳 Guanghua School of Stomatology, Hospital of Stomatology, Guangdong Provincial Key Laboratory of Stomatology, Sun Yat-Sen University, Guangzhou, Guangdong 510055, P.R. China

#Qi-Meng Li and Jin-Ling Li contributed equally to this study

Introduction

Human dental pulp cells (hDPCs) isolated from the postnatal human dental pulp comprise a heterogeneous mesenchymal cell population with the capacity to differentiate into odontoblast-like cells and to generate reparative dentine in response to exogenous stimuli or injury [1–3]. hDPCs can be a useful cell resource for developing biological treatment strategies for dental pulp repair and regeneration, and their therapeutic applications hinge on an understanding of the molecular mechanisms that induce odontogenic differentiation[4]. While growing evidence has demonstrated that signaling pathways, growth factors, and epigenetic regulators are involved in the odontogenic differentiation process of hDPCs [5–7]. Especially the epigenetic regulatory mechanisms underlying hDPC differentiation have attracted increasing attention. Recent evidence has illustrated that epigenetic modifications, such as histone acetylation and DNA (de)methylation, are involved in reparative dentinogenesis [8–14].

Histone methylation is a robust epigenetic mark that modifies the lysine and arginine residues of histone N-terminal tails and controls the accessibility of DNA at a particular locus by altering its chromatin compaction[15]. Histone methylation can signal either activation or repression, depending on the sites of methylation. Methylation at arginine residues, and di-/tri- Methylation at the H3K4, H3K36, and H3K79 are normally characterized as active marks, while methylation at the H3K9, H3K27, and H4K20 residues remain controversial [16,17]. The establishment and maintenance of histone methylation are dynamically regulated by site-specific histone methyltransferases (HMTs) and histone demethylases (HDMs), which play important roles in multiple cellular processes, including cell proliferation, differentiation, senescence, DNA damage response, oncogenesis and individual development [18–21]. During murine tooth germ development, covalent histone modifications characterized by H3K4me3 and H3K27me3 can be detected in the first molars of mouse embryos. In addition, several HMTs and HDMs are expressed in the mesenchyme and the epithelium of the tooth germ [22,23]. During the odontogenic differentiation of human dental pulp stem cells (hDPSCs), histone methylation levels in the promoters of mineralization markers, such as RUNX2 (RUNX family transcription factor 2, also known as CBFA1), MSX2, and DLX5, are altered, followed by the upregulation of gene expression levels[24]. This evidence suggests that histone methylation may be relevant to the odontogenic differentiation of dental-derived mesenchymal stem cells. However, little is known about how histone methylation controls the odontogenic differentiation of hDPCs.

In the present study, we investigated differentially expressed HMTs and HDMs during the odontogenic differentiation of hDPCs. The HDM KDM5A, also known as JARID1A/RBP2, was found to be highly expressed in the differentiated cells [25,26]. To determine the existence and function of KDM5A in the odontogenic differentiation of hDPCs, KDM5A expression was profiled during cell passaging and odontogenic induction. shRNA was then used to knock down KDM5A expression levels in hDPCs, and the role of KDM5A depletion in the odontogenic differentiation potentiality of hDPCs was estimated.

Materials and methods

Ethics committee approval and patient consent

This study was approved by the Ethics Committee of the Affiliate Stomatology Hospital of Sun Yat-sen University. Informed written consent was obtained from the donors. The investigation conformed to the principles outlined in the Declaration of Helsinki.

Cell isolation and culture

To obtain hDPCs, healthy human impacted third molars or premolars were collected from young adults aged 18 to 25 years in the Department of Oral and Maxillofacial Surgery at the Affiliate Stomatology Hospital of Sun Yat-sen University after informed patient consent was obtained according to ethical guidelines. hDPCs were isolated and cultivated as previously described[27]. Briefly, minced pulpal tissues were digested for 20 minutes at 37°C in a solution with 3 mg/mL

type I collagenase and 4 mg/mL dispase (Gibco, CA, USA) and were then cultured in Dulbecco's Modified Eagle Medium (DMEM) (Gibco) plus 10% fetal bovine serum (FBS) (Gibco), 100 units/mL penicillin and 100 mg/mL streptomycin (Gibco) at 37°C in a humidified atmosphere of 95% O_2 and 5% CO_2. Cells that migrated out of pulp pieces after 2 weeks were trypsinized, harvested and passaged serially. Cells collected at passage 2 or 3 were then used for further study.

Induction of odontogenic differentiation

For odontogenic differentiation, hDPCs were seeded into 24-well plates (2×10^4 cells per well) and 6-well plates (10^5 cells per well) and expanded in DMEM containing 10% FBS until they reached 80% confluence. The cells were then exposed to mineralization medium (MM), which contained DMEM supplemented with 5% FBS, 50 μg/L ascorbic acid, 10 mM β-glycerophosphate and $10^{-[7]}$ M dexamethasone (Sigma-Aldrich, St. Louis, MO, USA). Cells treated with growth medium (GM) were used as the control group. The culture medium was changed every 3 days.

Real-time qPCR

Total RNA was extracted from the hDPCs using TRIzol reagent (Life Technologies Corporation, CA, USA) following the manufacturer's protocol. Reverse transcription was performed using a Transcriptor First Strand cDNA Synthesis Kit (Roche, Basel, Switzerland). Real-time qPCR was performed using a LightCycler 480 with SYBR Green I Master (Roche). Specific primers were designed using Primer Express v3.0 software and were synthesized by Invitrogen (Life Technologies Corporation). The primer sequences are shown in Table 1. The housekeeping gene β-actin was used as a reference. Relative gene expression was calculated using the comparative $2^{-\Delta\Delta Ct}$ method. Each experiment was performed in triplicate.

Western blot analysis

Total proteins were harvested using RIPA lysis buffer with phenylmethylsulfonyl fluoride (PMSF, Beyotime Biotechnology, Haimen, China), while nucleoproteins were extracted with nuclear and cytoplasmic extraction reagents (Thermo Scientific, Rockford, IL, USA). Then, the concentrations of total proteins or nucleoproteins were measured with a bicinchoninic acid (BCA) protein assay (Beyotime Biotechnology). Equal amounts of protein were electrophoresed in a 4% ~ 20% Tris-Gly Mini Precast PAGE Gel (Hegao Biotechnology, Shanghai, China) and were then blotted onto polyvinylidene difluoride (PVDF) membranes (Millipore, Billerica, MA, USA). The membranes were incubated with the following primary antibodies overnight at 4°C: anti-KDM5A (Abcam, Cambridge, UK; 1:500), anti-DSPP (Santa Cruz Biotechnology, Santa Cruz, CA, USA; 1:200), anti-DMP1 (Abcam; 1:400), anti-OCN (Abcam; 1:1000), anti-OSX (Abcam; 1:1000), anti-H3K4me2 (Abcam; 1:500), anti-H3K4me3 (Abcam; 1:500), anti-H3 (Abcam;1:2000), and anti-β-actin (Bioworld, MN, USA; 1:5000). Then, the membranes were steeped in horseradish peroxidase (HRP)-conjugated anti-rabbit (Abcam; 1:2000) or anti-mouse (Abcam; 1:2000) secondary antibody for 1 hour at room temperature. Protein bands were visualized with an enhanced chemiluminescence system (Millipore ECL Western Blotting Detection System, Millipore), and band densities were obtained and normalized to β-actin using ImageJ 1.47 software (National Institutes of Health, MD, USA).

Alizarin red S staining

To assess mineralization *in vitro*, transfected cells seeded in 6-well plates were allowed to undergo odontogenic differentiation for 14 days. After culture, the cells were rinsed three times with PBS, fixed with 4% paraformaldehyde solution for 30 minutes and rinsed in distilled water. Mineral depositions were stained with 1% alizarin red S (GL Biochem, Shanghai, China) solution for 10 minutes at room temperature and were rinsed several times in distilled water. The mineralized nodules were then photographed. For quantitative analysis, the stains were dissolved with 10% cetyl-pyridinium chloride (CPC, Sigma-Aldrich) for 40 minutes, and the absorbance of the solution was measured at a wavelength of 562 nm using an automated microplate reader (Sunrise, Tecan, Salzburg, Switzerland). Quantitative measurements were calculated according to the generated standard curve.

Table 1. The primer sequences for real-time qPCR analysis.

β-actin	Forward	CTGCGGGTATCCATGAGA
	Reverse	TACCACCACTGAGAACGATG
ASH1 L	Forward	GATGTATCTACCGCTAAATCCCC
	Reverse	TAGTTTTTGAATCATTTACCTCT
DOT1	Forward	AAGAAGATGAACACTGCGAACCC
	Reverse	CGCTCGGAGGTAGCTGGTAGAAC
ESET(SEDB1)	Forward	GAAGCGTCAAGTGGCAGTAAAAT
	Reverse	TGATGTAGCAAGACTCCTCGCC
G9A	Forward	GGTCGTACAGAGTGGCATCAAGG
	Reverse	CGGGCATCTATGCAGTACACCT
MLL1	Forward	CCAGAAAATGAGAGTAATGATA
	Reverse	GCTAAGGGGATTGTTGGAGGCA
MLL2	Forward	GTTGTGTGACCTGTTCTTCTGT
	Reverse	CAAACCAACATCTTAGAGTCAT
MLL3	Forward	GTCACTGGAGAACTGAACGCAC
	Reverse	CCTGAATCCGAGACCGTGC
MLL4	Forward	GGATGACTTTGATGTAGTGGACGC
	Reverse	GATGGGGAACTTGTAGTCGTAGGT
MLL5	Forward	ATGTTCAGTCTTCACCTTCATCTCA
	Reverse	TTGAGCAGGAATTACAGATCCAGGT
NSD1	Forward	CCGCCAGACAGACTGCTCATT
	Reverse	AGGTCTATGAGATCCATCACCAAAG
PRMT1	Forward	GCACCCTCACTTACCGCAACT
	Reverse	TCTAACTTGTTGGCTTTGACGAT
PRMT4	Forward	CCAAGGCAGGGGACACGC
	Reverse	CAAGTCATAGGCGGTCGGCA
PRMT5(IBP72)	Forward	GAACCGTCCTCCACCTAATGC
	Reverse	TGATGGGGTCCTTTTCAAACACT
PRDM4	Forward	CAAATACCATCTCACCCGCC
	Reverse	AGAGACTCATCCGCTGAATACACA
PRDM12	Forward	TGGGAGGTGTTCAATGAGGAT
	Reverse	CCCCAGGAAGGTGTTGTGTGA
PRDM16	Forward	TTCCACCTTAGATTCTGAGGCTTTA
	Reverse	AAATGCTCCAGACTCCGACG
PTIP	Forward	AGTCGCTACACGGCATTCAGTC
	Reverse	CCGCAACCTCTCCACCAAG
SETD1A	Forward	ACCAACCTGACCACCCCAAA
	Reverse	GGCAAACAGACCCCACTCGT
SETD2	Forward	ACCCAGACAAGCAAACTCAAAAT
	Reverse	AACTTCCGGCGTTCCTCTG
SETD7	Forward	GCAAATCACTCCTTCACTCCAAAC
	Reverse	GGTCATAGCCATAGGCAACGG
SETD8	Forward	CAGCAGAACCTCCAAAAACTCC
	Reverse	TCTTCCTTCCCACTTTCAATCAA
SMYD2	Forward	CCACCAAGGACAAGGATAAGGC
	Reverse	AATGACGTTGCGTGCATATCTG
SMYD3	Forward	CCCAGTATCTCTTTGCTCAATCAC
	Reverse	ACGGAAACAGTCACATTCAAAGC
SUV39H1	Forward	CCATCTGGGACGCATCACT
	Reverse	CCTGGTCATTGTAGGCAAACTT
EZH2(KMT6A)	Forward	TCCGAGAGTGTGACCCTGACCT
	Reverse	ATAGATGCTTTTTGGAGCCCCG
KDM2A	Forward	CATAACCAACCGTTCCCACCTAA
	Reverse	GACAGAACGCCTGCTGCTCAA
KDM2B	Forward	GTGACATCTTTCTGGGAGACCGT
	Reverse	CTGGGTCACACAGTACACGTATCT
KDM3A	Forward	TGCCCGAGTACACAAGGCGAGAT
	Reverse	TCCCACATAGACCATGACATTAG
KDM3B	Forward	ATCTCTCTAACACTCATACAAATCA
	Reverse	TAGGACCTTGCCAGTTTGGATTCAT
KDM4A	Forward	TGGACCTCTACAGCATCAACTACC
	Reverse	CATATTTCTTCAGCATTAACGGGG
KDM4B	Forward	GTCATCACCAAGAACCGCAACG
	Reverse	CAGCTGGACACAGTCCCTACTC
KDM4 C	Forward	AAGACTAAGCCCCTCATACCAGA

(*Continued*)

Table 1. (Continued).

	Reverse	CATAACAACTTGCATGAACCCGT
KDM4D	Forward	ATTCCCTTCAATCGCATAACTCA
	Reverse	CTTGTCCATCAAAGCCCCAT
KDM5A	Forward	TTACCAACAGGTCAGACGCAT
	Reverse	GGTTTGCTACATTCCTCGGCG
KDM5B	Forward	TTGTCCCCATTGTCGGAGGTC
	Reverse	TTACTTTCGGCTTGGTGCGTC
KDM5 C	Forward	GTGAGCGGAGGTTTCCTAATA
	Reverse	GGCGCAAGGCAGGTTGTT
KDM6A	Forward	GGACAAGTTGAATCCACCTACACC
	Reverse	AGAGCTCCAGCAAGGCCACGTATT
KDM6B	Forward	TACACCTTGAGCACAAACGGA
	Reverse	AGCCTCTCCTTCGCTTGCCTC
JMJD1 C	Forward	AAACCCCATAATAATGAGAAGGCAG
	Reverse	GAGTGTCAACAGACTTCCGCTTC
JMJD5	Forward	CCATCCTGGGGGACATCCTTCTTA
	Reverse	ACCAAAAACTGCTCCCTGAAATGC
JMJD6	Forward	GTGGCATGTTGTCCTCAATCTC
	Reverse	TTTGGTCTCCCTCTTACCGTCT
LSD1	Forward	TAAAACCCCTACCAACTAAAAAG
	Reverse	ATGTGGCAACTCGTCCACCCAC
PHF2	Forward	CCCCGACGAGCCCTGGTGTGTTC
	Reverse	CTCACCGTCATCCGACACGTACT
PHF8	Forward	TCTCGGCGAACCAAGATAGCA
	Reverse	TTGGTCTTATTATCAGGGTCGCC
KIAA1718	Forward	AACTTCCCCATACCATTCCCGA
	Reverse	CATTTGTCAGCAGTAATCGTAG
NO66	Forward	TCTACCGCTGACCTGGATTCG
	Reverse	CCTGCGGACAGAGGAGACG
DSPP	Forward	CCAGTTCCTCAAAGCAAACC
	Reverse	GGCATTTAACTCATCCTGTACTGA
DMP1	Forward	CTCCGAGTTGGACGATGAGG
	Reverse	TCATGCCTGCACTGTTCATTC
RUNX2	Forward	ACCATGGTGGAGATCATCGC
	Reverse	CATCAAGCTTCTGTCTGTGC
OSX	Forward	GCCAGAAGCTGTGAAACCTC
	Reverse	GCTGCAAGCTCTCCATAACC
OCN	Forward	AGCAAAGGTGCAGCCTTTGT
	Reverse	GCGCCTGGGTCTCTTCACT
DSPP (ChIP)	Forward	CCAGTTCCTCAAAGCAAACC
	Reverse	GGCATTTAACTCATCCTGTACTGA
DMP1 (ChIP)	Forward	CTCCGAGTTGGACGATGAGG
	Reverse	TCATGCCTGCACTGTTCATTC
OSX (ChIP)	Forward	ACCATGGTGGAGATCATCGC
	Reverse	CATCAAGCTTCTGTCTGTGC
OCN (ChIP)	Forward	GCCAGAAGCTGTGAAACCTC
	Reverse	GCTGCAAGCTCTCCATAACC

Establishment of stable KDM5A knockdown by shRNA in hDPCs

KDM5A knockdown was performed by shRNA in hDPCs. The lentivirus vector hU6-MCS-CMV-Puromycin, containing either KDM5A shRNA (5′-GCCAAGAAC ATTCCAGCCTTT-3′) or negative control shRNA, was obtained from GeneChem Biotechnologies (Shanghai, China). The lentiviral vectors were transfected into 293 T cells with the psPAX2, pMD.2 G packaging plasmid mix in serum-free Opti-MEM using the Lipofectamine 3000 reagent (Invitrogen Co, Carlsbad, CA, USA). The transfection mix was replaced with fresh DMEM plus 10% FBS 6 hours after transfection. The viruses were then harvested, filtered, and used to transfect hDPCs. Transfected hDPCs were selected with 1 μg/mL puromycin 3 days after virus infection. The stable clones were then maintained in 0.25 μg/mL puromycin to ensure a transfection rate greater than 90%. Knockdown was confirmed using real-time quantitative polymerase chain reaction (real-time qPCR) and western blot analysis.

Alkaline phosphatase (ALP) activity analysis

Transfected cells seeded into 24-well plates underwent odontogenic differentiation for 7 and 14 days as described above. The ALP activity of the hDPCs was then detected by utilizing an ALP assay kit (Nanjing Jiancheng Bioengineering Institute, Nanjing, China) according to the manufacturer's protocol. Briefly, cells were lysed with 0.1% Triton X-100 in 10 mM TrisHCl at 4°C overnight, and the absorbance of the solution was measured at 520 nm using an automated microplate reader (Sunrise). The total protein content in each individual sample was quantified with a BCA protein assay (Beyotime Biotechnology), and ALP activity was normalized to the total protein content.

Chromatin immunoprecipitation (ChIP) and qRT-PCR analysis

The promoters of DSPP, DMP1, OCN, OSX and H3K4me3 marks from the Encyclopedia of DNA Elements (ENCODE) were retrieved using UCSC Genome Browser (http://genome.ucsc.edu/cgi-bin). Primers specific to these regions with H3K4me3 enrichment were designed using Primer Express v3.0 software (Table 1) and were synthesized by BGI Technology (BGI, Shenzhen, China). For the ChIP assay, the EZ-Magna ChIP™ G Chromatin Immunoprecipitation Kit (Millipore) was utilized according to the manufacturer's instructions. Approximately 1×10^7 transfected cells cultured in MM for 14 days were crosslinked with 1% formaldehyde (Sigma-Aldrich). Cells were then lysed and fragmented using a Dounce homogenizer and sheared by an ultrasonic processor (Sonics, Newtown, USA). The chromatin was then subjected to IP using 5 μg of H3K4me3-specific antibody (Abcam) overnight at 4°C with rotation. After washing, the protein-DNA cross-links were reversed, and the DNA was purified. qRT-PCR was performed to validate the sequences of interest with the primers. Normal rabbit IgG served as a negative control for IP.

Statistical analyzes

All experiments were repeated at least in triplicate. Experimental results are presented as the mean ± standard deviation (SD). The data were analyzed using the SPSS 19.0 software program (SPSS, Chicago, IL, USA). Student's t-test was used to compare two normally distributed groups. For multiple comparisons, the data passed normality and equal variance tests and were then subjected to one-way analysis of variance (one-way ANOVA) and the Student-Newman-Keuls multiple comparison test. Significantly different levels were set at the 95% and 99% confidence intervals and are marked with *($P < 0.05$) and ** ($P < 0.01$), respectively.

Results

Odontogenic differentiation and HMT/HDM expression in hDPCs

To ensure the odontogenic differentiation of hDPCs, the expression levels of the odontoblast markers DSPP (Dentin Sialophosphoprotein) and DMP1 (Dentin Matrix Protein 1) and mineralized matrix deposition were assessed after mineralization induction. As shown in Figure 1(a,b), the expression levels of DSPP and DMP1 were upregulated, and the mineralized matrix deposition also increased after induction.

To investigate potential roles of histone methylation in the differentiation process of hDPCs and to identify the expression levels of the HMTs and HDMs during hDPC odontogenic differentiation, the mRNA expression levels of 25 HMTs and 21 HDMs were profiled in cells cultured in MM or GM for 14 days. Real-time qPCR revealed that eight enzymes were expressed differentially during the hDPC odontogenic differentiation process. The expression levels of 4 HMTs (PRDM12, SETD1A, SUV39H1, and EZH2) and 3 HDMs (KDM2B, KDM5 C, and JMJD6) decreased after mineralization induction; the HDM KDM5A was the only enzyme of those assessed that was induced after odontogenic differentiation (Figure 1(c,d)).

Expression features of the histone demethylase KDM5A in hDPCs

To evaluate the expression profiles of KDM5A in hDPCs during continuous passaging *in vitro*, the mRNA and protein expression levels of KDM5A in cells from the 1st to 8th passages were detected by
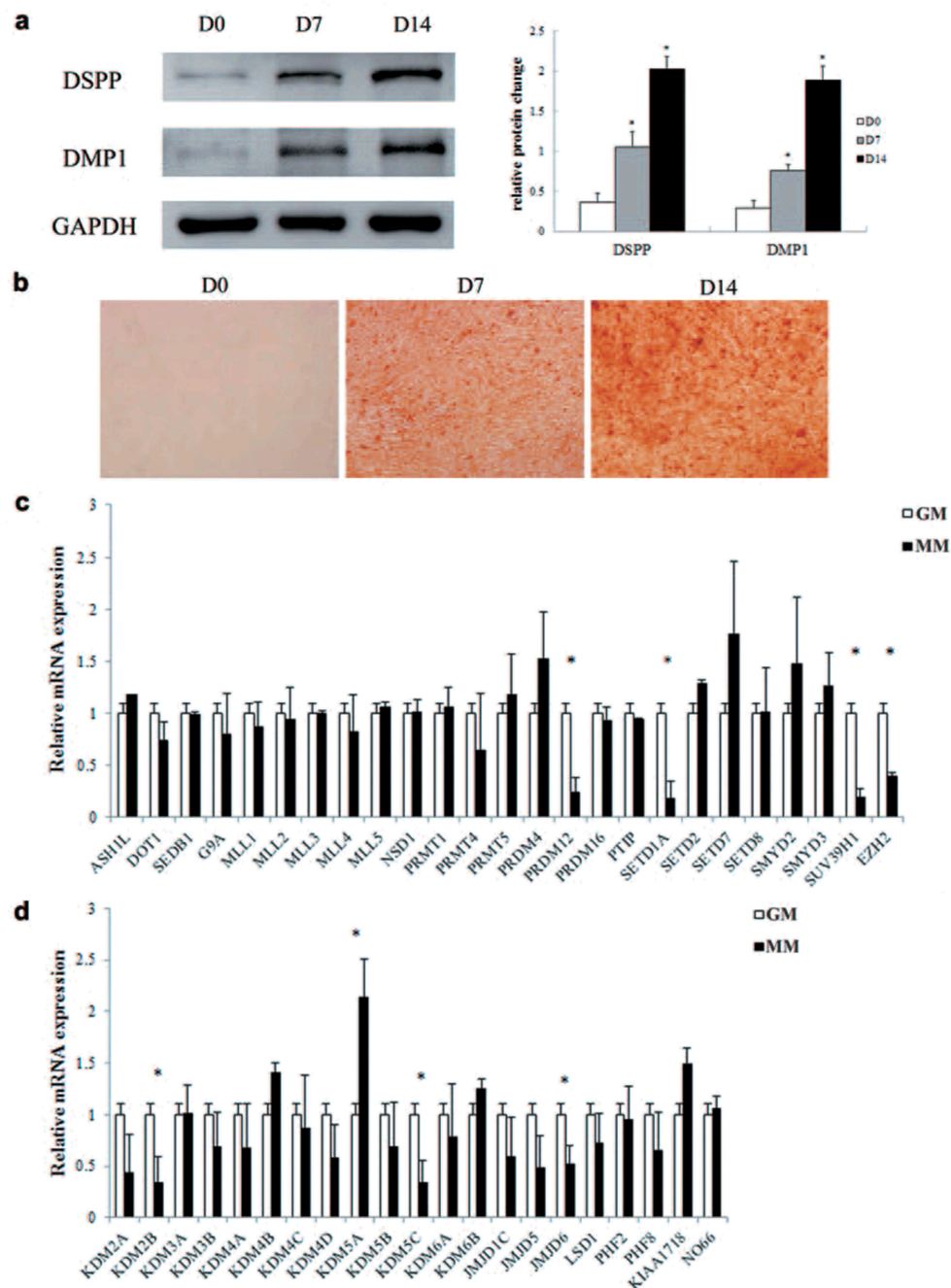
Figure 1. Differential HMT and HDM expression during the odontogenic differentiation of hDPCs.

(a) The expression levels of DSPP and DMP1 were assessed using western blot analysis on days 0, 7, and 14 of culture in MM. GAPDH was used as an internal control. **(b)** The formation of mineralized nodules was assessed using alizarin red S staining (100X). **(c)** HMT mRNA expression was assessed by real-time qPCR. **(d)** HDM mRNA expression was assessed by real-time qPCR. The mRNA level of each product was normalized to the β-actin mRNA level. GM: growth medium; MM: odontogenic differentiation medium. All results are presented as the mean ± SD of three independent experiments. Procedures were performed as described in the text (n = 3). *$P < 0.05$.

using real-time qPCR and western blot, respectively. The expression level of KDM5A was elevated in the 1st and 2nd passages, maintained stably at a high level in the 3rd to 6th passages, and then decreased in the 7th and 8th passages (Figure 2(a,b)).

To examine the alterations to KDM5A expression during odontogenic differentiation, the mRNA and protein levels of KDM5A were analyzed in hDPCs induced to undergo odontogenic differentiation for 7 and 14 days. The results
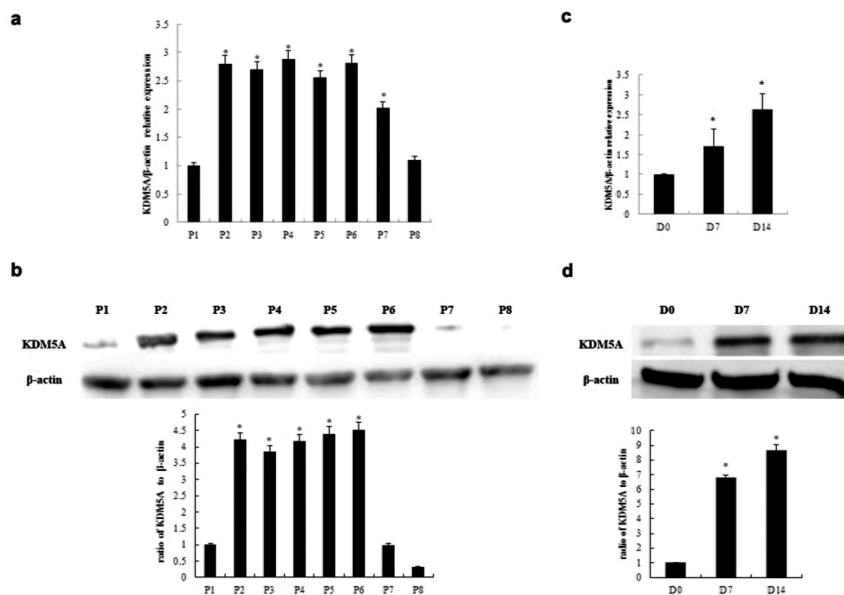
Figure 2. Histone demethylase KDM5A expression in hDPCs.

(a) Real-time qPCR analysis of KDM5A mRNA expression at different passages. The amount of each product was normalized to β-actin. **(b)** The protein expression levels of KDM5A in the hDPCs at different passages were assessed by western blot analysis and densitometric evaluation (expressed as the ratio of KDM5A to β-actin). β-actin was used as an internal control. **(c)** KDM5A mRNA expression levels in hDPCs in MM for 0, 7 and 14 days were measured using real-time qPCR. The amount of each product was normalized to β-actin. **(d)** KDM5A protein expression levels in hDPCs in MM for 0, 7 and 14 days were assessed by western blot analysis and densitometric evaluation (expressed as the ratio of KDM5A to β-actin). β-actin was used as an internal control. All results are presented as the mean ± SD of three independent experiments. Procedures were performed as described in the text (n = 3). *P < 0.05.

showed that KDM5A increased in a time-dependent manner during odontogenic induction (Figure 2(c,d)).

Effects of KDM5A knockdown on the mineralization potentiality of hDPCs

To explore the role of KDM5A in hDPC odontogenic differentiation, KDM5A was knocked down using shRNA. hDPCs without transfection were used as the normal control group to exclude the possibility that the properties of hDPCs might be affected by the lentivirus vector. Real-time qPCR and western blot analysis showed almost 70% depletion of KDM5A in the target shRNA group relative to that in control shRNA group, suggesting that KDM5A was effectively knocked down in hDPCs. There was no difference between the normal control group and control shRNA group (Figure 3(a,b)).

ALP activity and the formation of mineralized nodules were then examined in KDM5A-shRNA cells under normal culture conditions (GM

group) and in MM (MM group). As shown in Figure 3(c), KDM5A silencing enhanced ALP activity relative to that of the control group under both normal culture and induction conditions. Furthermore, KDM5A knockdown increased the number of mineralized nodules after treatment with mineralization induction for 14 days, as assessed by alizarin red S staining. Under normal culture conditions, there was no significant difference in the number of mineralized nodules between the KDM5A-shRNA and the control group (Figure 3(d)).

Effects of KDM5A knockdown on odontogenic differentiation markers in hDPCs

To further investigate the differentiation potential of hDPCs after KDM5A knockdown, the mRNA levels of several matrix-related genes (DMP1, DSPP, RUNX2, OSX, and OCN) were detected after the cells were cultured in MM or GM for 14 days. As shown in Figure 4, KDM5A depletion significantly enhanced DMP1, DSPP, OSX (Zinc
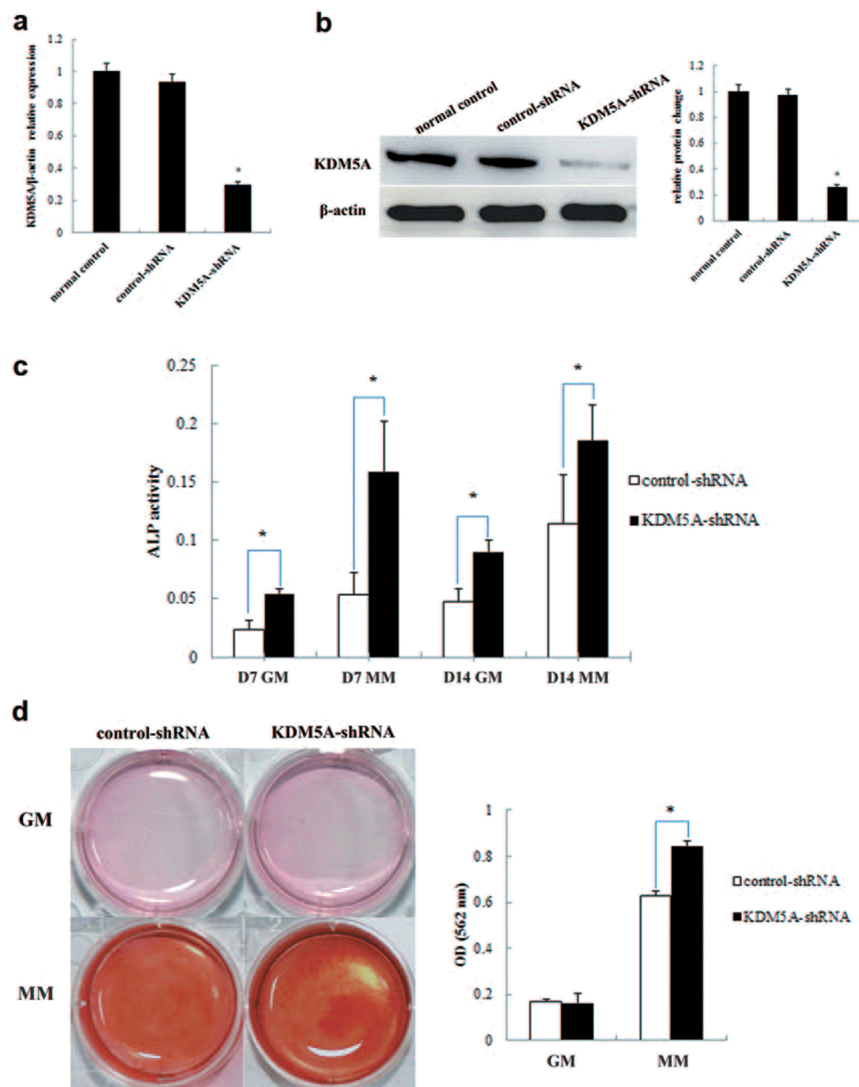
Figure 3. Effects of KDM5A knockdown on the mineralization potentiality of hDPCs.
(a) Real-time qPCR analysis of KDM5A mRNA expression in KDM5A-shRNA- transfected, control-shRNA-transfected, and normal hDPCs. The amount of each product was normalized to β-actin. **(b)** The protein expression levels of KDM5A in KDM5A-shRNA-transfected, control-shRNA-transfected, and normal hDPCs were assessed by western blot analysis and densitometric evaluation (expressed as the ratio of KDM5A to β-actin). β-actin was used as an internal control. **(c)** Cells were cultured for 7 and 14 days in GM or MM, and ALP activity was measured. **(d)** Mineralization was analyzed using alizarin red S staining on day 14. The histogram shows the quantification of mineralization by densitometry. All results are presented as the mean ± SD of three independent experiments. Procedures were performed as described in the text (n = 3). *$P < 0.05$.

finger protein osterix, also known as transcription factor Sp7), and OCN (Osteocalcin, also known as OC or Bone Gamma-Carboxyglutamate Protein, BGLAP) expression (Figure 4(a)). No significant difference was found for RUNX2 in neither the MM nor the GM group. Western blotting was performed to confirm the significant results obtained by real-time qPCR (Figure 4(b)), which verified the upregulation of odontogenic

differentiation markers in cells undergoing odontogenic induction (cultured in MM).

Effects of KDM5A knockdown on the methyl marks of H3K4 in hDPCs

Since KDM5A is a histone demethylase specific for tri- and dimethylated H3K4, the methyl marks of H3K4 were observed using western blot. As shown
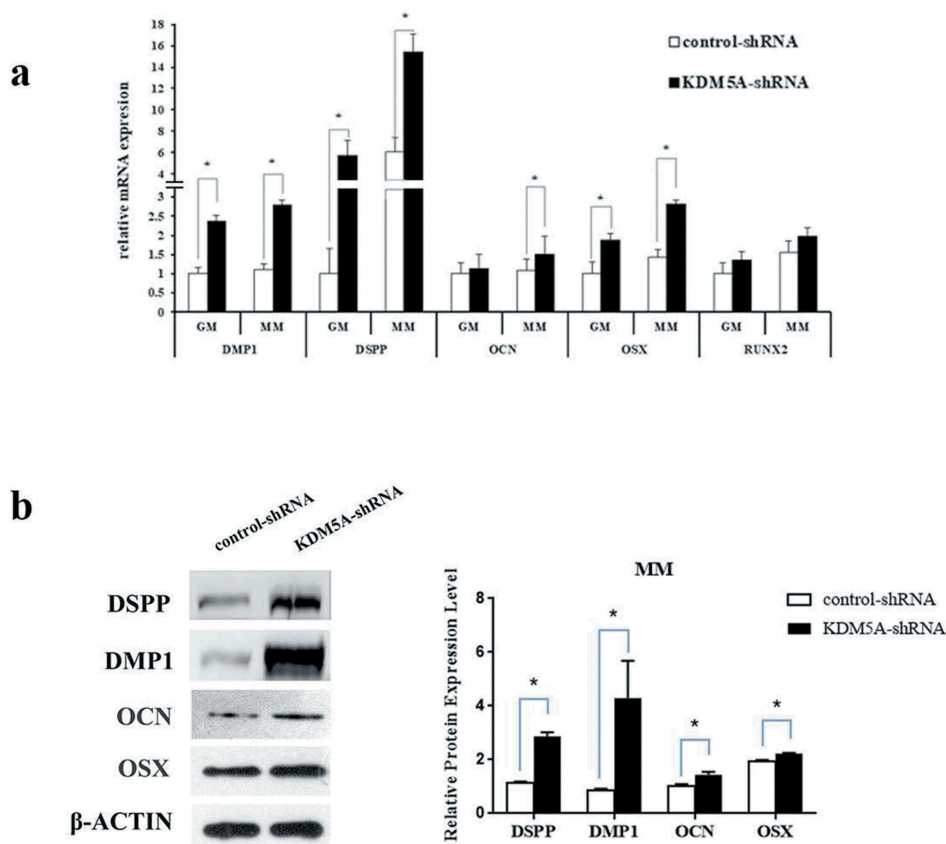
Figure 4. Effects of KDM5A knockdown on the odontogenic differentiation markers of hDPCs.

(a) Cells were cultured for 14 days in GM or MM. DMP1, DSPP, RUNX2, OSX, and OCN mRNA expression levels were detected using real-time qPCR. The amount of each product was normalized to β-actin. **(b)** Cells were cultured for 14 days in MM. DSPP, DMP1, OSX, OCN protein expression levels were detected using western blot and densitometric evaluation (expressed as the ratio to β-actin). The expression of β-actin was used as an internal control. All results are presented as the mean ± SD of three independent experiments. Procedures were performed as described in the text (n = 3). *$P < 0.05$.

in Figure 5(a), H3K4me3 increased in the KDM5A-shRNA group, whereas no significant difference was found for H3K4me2. Next, ChIP-PCR was implemented to determine whether KDM5A knockdown altered the modification of H3K4me3 on the promoters of odontogenic differentiation markers. The results revealed that KDM5A depletion prompted a significant increase in H3K4me3 levels on the promoters of DSPP, DMP1, OCN, and OSX (Figure 5(b)).

Discussion

Histone methylation is essential for many biological processes, such as transcriptional regulation, X-chromosome inactivation and heterochromatin formation [18,28]. It regulates gene expression and forms part of the epigenetic memory system, which modulates cell differentiation in embryonic

stem cells (ESCs), human bone marrow mesenchymal stem cells (MSCs), hDPSCs, and oncocytes [29–32]. Osteo/odontogenic differentiation is likely modulated by histone methylation. Gopinathan et al [24]. reported that early mineralization genes (i.e., RUNX2, MSX2, and DLX5) are predominantly marked with H3K4me3 active marks, while late mineralization markers (i.e., OSX, IBSP, and BGLAP) are enriched for H3K9me3 or H3K27me3 inactive marks in dental pulp progenitors and dental follicle progenitors. Increased enrichment for H3K4me3 correlates with increased expression levels of BMP2, BMP4, DLX5, and RUNX2 in both cell types during mineralization induction. Zheng et al. [22] demonstrated that the bivalent modifications characterized by H3K4me3 and H3K27me3 can be detected during murine tooth germ development. The methyltransferases SET7 and EZH2 and

a

b

ChIP-PCR
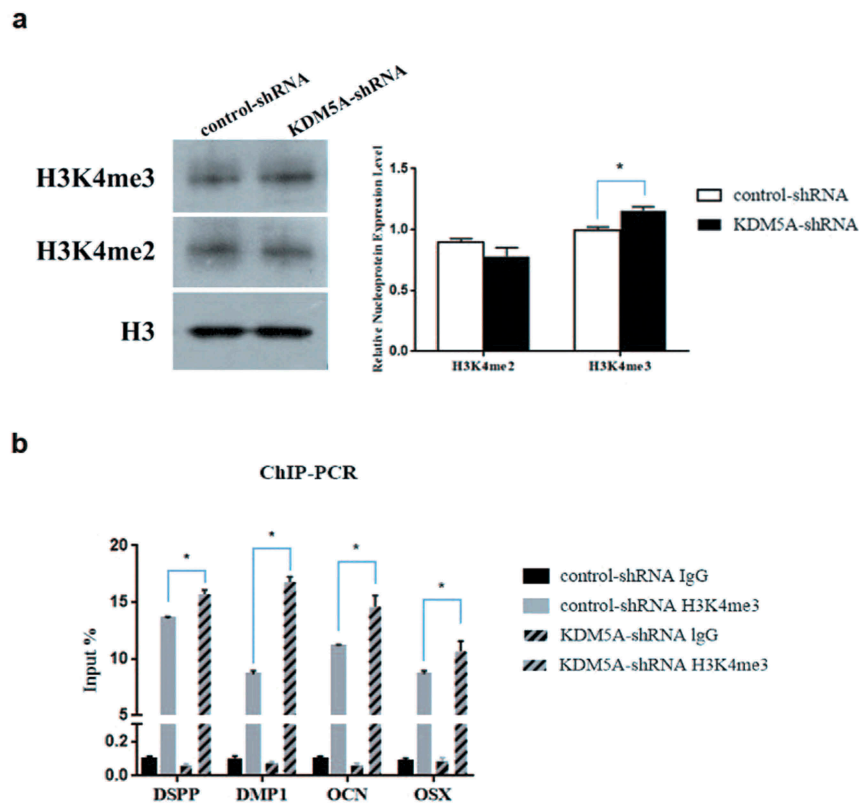
Figure 5. Effects of KDM5A knockdown on methyl marks of H3K4 in hDPCs.
(a) Cells were cultured for 14 days in MM. H3K4me3/me2 levels were detected using western blot and densitometric evaluation (expressed as the ratio to H3). **(b)** Signals of H3K4me3 IP-DNA relative to the total amount of input DNA in hDPCs were extracted from the control group (no stripes) and KDM5A-knockdown group (stripes), as analyzed by qPCR using specific primer pairs for odontogenic differentiation markers. All results are presented as the mean ± SD of three independent experiments. Procedures were performed as described in the text (n = 3). *$P < 0.05$.

demethylases KDM5B and JMJD3 are expressed in a spatial-temporal manner. A recent study reported that four H3K9 methyltransferases (G9A, SETDB1, SUV39H1, and PRDM2) are highly expressed in the mesenchyme of the tooth germ in mice[23]. These studies suggested that histone methylation might play active roles in the differentiation and lineage commitment of dental mesenchymal stem cells. However, no data on the expression patterns and functions of the HMTs or HDMs in the odontogenic differentiation process of hDPCs are available. In the present study, we identified the expression profiles of HMTs and HDMs in hDPCs induced to undergo odontogenic differentiation. The expression levels of four HMTs (PRDM12, SETD1A, SUV39H1, and EZH2) and three HDMs (KDM2B, KDM5 C, and JMJD6) decreased after mineralization induction; KDM5A was the only enzyme that was induced after odontogenic differentiation. KDM5A has

been reported to play important roles in the osteogenic differentiation process [33,34]. Thus, KDM5A was identified for its regulatory role in the odontogenic differentiation of hDPCs.

KDM5A (JARID1A/RBP2), originally identified by virtue of its capacity to bind the retinoblastoma protein (pRB), is a member of the JmjC-containing JARID1 protein family, which is characterized by its ability to selectively remove methyl marks from H3K4 [26,35]. KDM5A has been detected in multiple cell lines, such as ESCs, human adipose-derived stem cells (hASCs), spermatogonial stem cells, and oncocytes originating from numerous tissues [33,36–39]. In the present study, KDM5A mRNA and protein were detected in primary hDPCs, and their expression levels gradually increased in early passages and then decreased in later passages when the cells were serially passaged. It is possible that KDM5A expression is elevated in hDPCs undergoing proliferation and

early spontaneous differentiation (from 1st to 6th passage), whereas its expression is attenuated following cell senescence (at 7th or 8th passage) by morphological abnormalities and self-renewal defects. Furthermore, its expression was also promoted during odontogenic differentiation. This result was consistent with the report that KDM5A is upregulated in leukemic HL60 cells with differentiation[40].

KDM5A has been reported to play important roles in controlling stemness and the differentiation fates of stem cells. In ESCs, it cooperates with KLF4 to promote the transcriptional activation of OCT4[36]. KDM5A is required to maintain the repressive state of genes involved in cell development, including the Wnt5a, Irx3, Igf2, and Hox genes, and KDM5A displaces from the promoters of related genes when ESCs are induced to undergo differentiation [41,42]. In hASCs, KDM5A physically and functionally interacts with RUNX2 and represses its transcriptional activity. The hypoactivity of RUNX2 then decreases the expression of the OSX and OCN genes. On the other side, KDM5A can directly repress OCN through its H3K4 demethylase activity. When hASCs are induced to osteogenic differentiation, KDM5A occupancy decreases dramatically, and its depletion enhances osteogenic differentiation [33,34]. According to these previous studies, KDM5A seemingly tends to maintain pluripotent status by inducing stem cell-specific genes and alleviate cell differentiation by reducing the expression of lineage genes. In the present study, after identifying KDM5A expression patterns in hDPCs, KDM5A was knocked down to explore its role in the odontogenic differentiation potential of hDPCs. ALP activity and mineralized nodule formation were analyzed under normal culture and induction conditions. ALP activity was enhanced under both conditions, and mineralized nodule formation was increased in KDM5A-knockdown cells in response to odontogenic induction for 14 days relative to the control group, but no significant differences were detected under normal culture conditions between the two groups. These findings were further confirmed by the increased expression levels of DMP1, DSPP, OSX, and OCN in cells undergoing mineralization induction. These results indicated that KDM5A

was negatively correlated with the odontogenic differentiation of hDPCs, consistent with the current understanding of its repressive effect on cell differentiation.

KDM5A is a histone demethylase specific for tri- and dimethylated H3K4; hence, ectopic expression of KDM5A reduces global levels of H3K4me3/me2 [41,43]. KDM5A has been suggested to function as a transcriptional repressor by binding to its target-gene promoter and to play an important role in cell differentiation. During NK cell activation, KDM5A binds to the suppressor of cytokine signaling 1 (SOCS1) promoter region, leading to a substantial decrease in its H3K4me3 modification and gene transcription[44]. Wang et al. reported that overexpression of KDM5A in MSCs inhibited BMP2-induced osteogenesis by decreasing H3K4me3 levels on promoters of RUNX2[45]. Knockdown of KDM5A resulted in significant increases in ALP, OCN and OSX expression in hASCs, since the levels of H3K4me3 on the promoters of OSX and OCN were maintained with lower KDM5A occupation[33]. In this study, KDM5A deficiency led to a significant increase in total H3K4me3 levels, whereas no significant difference was found for H3K4me2 in hDPCs induced to undergo odontogenic differentiation. To explore whether the enhanced levels of H3K4me3 in hDPCs were reflected in the upregulated odontogenic differentiation markers, ChIP-PCR was utilized to observe the H3K4me3 marks on the individual promoters of these genes. As expected, H3K4me3 levels on the promoters of DSPP, DMP1, OCN and OSX increased after KDM5A knockdown in hDPCs. These results revealed that KDM5A-dependent histone demethylation decreased the H3K4me3 marks on the promoters of matrix-related genes and impaired their expression, thereby restraining hDPC differentiation.

In conclusion, the present study estimated differentially expressed HMTs and HDMs during the odontogenic differentiation of hDPCs and demonstrated that KDM5A was highly expressed in odontogenically differentiated hDPCs. During an investigation into the role of KDM5A in regulating odontogenic differentiation, the results showed that KDM5A inhibited the odontogenic differentiation potentiality of hDPCs through its ability to remove H3K4me3 from specific gene promoters. These findings provide the first indication that histone

methylation is involved in the process of odontogenic differentiation in hDPCs and might have potentially innovative implications for the field of regenerative endodontics and pulp regeneration.

Highlights

(1) The expression levels of HMTs and HDMs were profiled in hDPCs.
(2) HDM KDM5A expression increased during early passages and mineralization induction.
(3) KDM5A depletion promoted odontogenic differentiation potentiality of hDPCs.
(4) KDM5A knockdown upregulated H3K4me3 on promoters of mineralization markers.

Disclosure statement

The authors declare that there are no conflicts of interest.

Funding

References

[1] Gronthos S, Brahim J, Li W, et al. Stem cell properties of human dental pulp stem cells. J Dent Res. 2002 Aug;81(8):531–535.

[2] Takeda T, Tezuka Y, Horiuchi M, et al. Characterization of dental pulp stem cells of human tooth germs. J Dent Res. 2008 Jul;87(7):676–681.

[3] Tamaoki N, Takahashi K, Tanaka T, et al. Dental pulp cells for induced pluripotent stem cell banking. J Dent Res. 2010 Aug;89(8):773–778.

[4] Kawashima N. Characterisation of dental pulp stem cells: a new horizon for tissue regeneration? Arch Oral Biol. 2012 Nov;57(11):1439–1458.

[5] Thesleff I. Epithelial-mesenchymal signalling regulating tooth morphogenesis. J Cell Sci. 2003 May 1;116(Pt 9):1647–1648.

[6] Lee SI, Kim DS, Lee HJ, et al. The role of thymosin beta 4 on odontogenic differentiation in human dental pulp cells. PLoS One. 2013;8(4):e61960.

[7] Yang F, Xu N, Li D, et al. A feedback loop between RUNX2 and the E3 ligase SMURF1 in regulation of differentiation of human dental pulp stem cells. J Endod. 2014 Oct;40(10):1579–1586.

[8] Wang T, Liu H, Ning Y, et al. The histone acetyltransferase p300 regulates the expression of pluripotency factors and odontogenic differentiation of human dental pulp cells. PLoS One. 2014;9(7):e102117.

[9] Zeng L, Zhao N, Li F, et al. miR-675 promotes odontogenic differentiation of human dental pulp cells by epigenetic regulation of DLX3. Exp Cell Res. 2018 Jun 1;367(1):104–111.

[10] Duncan HF, Smith AJ, Fleming GJ, et al. Histone deacetylase inhibitors epigenetically promote reparative events in primary dental pulp cells. Exp Cell Res. 2013 Jun 10;319(10):1534–1543.

[11] Li Q, Rao L, Zhang D, et al. Expression features of DNA methylcytosine dioxygenase ten-eleven translocation 1 in human dental pulp cells. J Endod. 2014 Nov;40(11):1791–1795.

[12] Rao LJ, Yi BC, Li QM, et al. TET1 knockdown inhibits the odontogenic differentiation potential of human dental pulp cells. Int J Oral Sci. 2016 Jun 30;8 (2):110–116.

[13] Zhang D, Li Q, Rao L, et al. Effect of 5-Aza-2⬚-deoxycytidine on odontogenic differentiation of human dental pulp cells. J Endod. 2015 May;41(5):640–645.

[14] Li Q, Yi B, Feng Z, et al. FAM20C could be targeted by TET1 to promote odontoblastic differentiation potential of human dental pulp cells. Cell Prolif. 2018 Apr;51 (2):e12426.

[15] Kouzarides T. Chromatin modifications and their function. Cell. 2007 Feb 23;128(4):693–705.

[16] Zhang Y, Reinberg D. Transcription regulation by histone methylation: interplay between different covalent modifications of the core histone tails. Genes Dev. 2001 Sep 15;15(18):2343–2360.

[17] Black JC, Van Rechem C, Whetstine JR. Histone lysine methylation dynamics: establishment, regulation, and biological impact. Mol Cell. 2012 Nov 30;48 (4):491–507.

[18] Barth TK, Imhof A. Fast signals and slow marks: the dynamics of histone modifications. Trends Biochem Sci. 2010 Nov;35(11):618–626.

[19] Tian X, Zhang S, Liu HM, et al. Histone lysine-specific methyltransferases and demethylases in carcinogenesis: new targets for cancer therapy and prevention. Curr Cancer Drug Targets. 2013 Jun;13(5):558–579.

[20] Hofstetter C, Kampka JM, Huppertz S, et al. Inhibition of KDM6 activity during murine ESC differentiation induces DNA damage. J Cell Sci. 2016 Feb 15;129 (4):788–803.

[21] Dutta A, Le Magnen C, Mitrofanova A, et al. Identification of an NKX3.1-G9a-UTY transcriptional regulatory network that controls prostate differentiation. Science. 2016 Jun 24;352(6293):1576–1580.

[22] Zheng LW, Zhang BP, Xu RS, et al. Bivalent histone modifications during tooth development. Int J Oral Sci. 2014 Dec;6(4):205–211.

[23] Kamiunten T, Ideno H, Shimada A, et al. Coordinated expression of H3K9 histone methyltransferases during tooth development in mice. Histochem Cell Biol. 2015 Mar;143(3):259–266.

[24] Gopinathan G, Kolokythas A, Luan X, et al. Epigenetic marks define the lineage and differentiation potential of two distinct neural crest-derived intermediate odontogenic progenitor populations. Stem Cells Dev. 2013 Jun 15;22(12):1763–1778.

[25] Defeo-Jones D, Huang PS, Jones RE, et al. Cloning of cDNAs for cellular proteins that bind to the retinoblastoma gene product. Nature. 1991 Jul 18;352 (6332):251–254.

[26] Takeuchi T, Watanabe Y, Takano-Shimizu T, et al. Roles of jumonji and jumonji family genes in chromatin regulation and development. Dev Dyn. 2006 Sep;235(9):2449–2459.

[27] Gronthos S, Mankani M, Brahim J, et al. Postnatal human dental pulp stem cells (DPSCs) in vitro and in vivo. Proc Natl Acad Sci U S A. 2000 Dec 5;97 (25):13625–13630.

[28] Bannister AJ, Kouzarides T. Reversing histone methylation. Nature. 2005 Aug 25;436(7054):1103–1106.

[29] Bernstein BE, Mikkelsen TS, Xie X, et al. A bivalent chromatin structure marks key developmental genes in embryonic stem cells. Cell. 2006 Apr 21;125(2):315–326.

[30] Ye L, Fan Z, Yu B, et al. Histone demethylases KDM4B and KDM6B promotes osteogenic differentiation of human MSCs. Cell Stem Cell. 2012 Jul 6;11(1):50–61.

[31] Du J, Ma Y, Ma P, et al. Demethylation of epiregulin gene by histone demethylase FBXL11 and BCL6 corepressor inhibits osteo/dentinogenic differentiation. Stem Cells. 2013 Jan;31(1):126–136.

[32] Maizels Y, Elbaz A, Hernandez-Vicens R, et al. Increased chromatin plasticity supports enhanced metastatic potential of mouse melanoma cells. Exp Cell Res. 2017 Aug 15;357(2):282–290.

[33] Ge W, Shi L, Zhou Y, et al. Inhibition of osteogenic differentiation of human adipose-derived stromal cells by retinoblastoma binding protein 2 repression of RUNX2-activated transcription. Stem Cells. 2011 Jul;29(7):1112–1125.

[34] Lv L, Liu Y, Zhang P, et al. The nanoscale geometry of TiO2 nanotubes influences the osteogenic differentiation of human adipose-derived stem cells by modulating H3K4 trimethylation. Biomaterials. 2015 Jan;39:193–205.

[35] Klose RJ, Yan Q, Tothova Z, et al. The retinoblastoma binding protein RBP2 is an H3K4 demethylase. Cell. 2007 Mar 9;128(5):889–900.

[36] Wang WP, Tzeng TY, Wang JY, et al. The EP300, KDM5A, KDM6A and KDM6B chromatin regulators cooperate with KLF4 in the transcriptional activation of POU5F1. PLoS One. 2012;7(12):e52556.

[37] Cao J, Liu Z, Cheung WK, et al. Histone demethylase RBP2 is critical for breast cancer progression and metastasis. Cell Rep. 2014 Mar 13;6(5):868–877.

[38] Nishio H, Hayashi Y, Moritoki Y, et al. Distinctive changes in histone H3K4 modification mediated via Kdm5a expression in spermatogonial stem cells of cryptorchid testes. J Urol. 2014 May;191(5 Suppl):1564–1572.

[39] Zhou M, Zeng J, Wang X, et al. Histone demethylase RBP2 decreases miR-21 in blast crisis of chronic myeloid leukemia. Oncotarget. 2015 Jan 20;6(2):1249–1261.

[40] Ge Z, Li W, Wang N, et al. Chromatin remodeling: recruitment of histone demethylase RBP2 by Mad1 for transcriptional repression of a Myc target gene, telomerase reverse transcriptase. Faseb J. 2010 Feb;24 (2):579–586.

[41] Christensen J, Agger K, Cloos PA, et al. RBP2 belongs to a family of demethylases, specific for tri-and dimethylated lysine 4 on histone 3. Cell. 2007 Mar 23;128(6):1063–1076.

[42] Pasini D, Hansen KH, Christensen J, et al. Coordinated regulation of transcriptional repression by the RBP2 H3K4 demethylase and polycomb-repressive complex 2. Genes Dev. 2008 May 15;22(10):1345–1355.

[43] Torres IO, Kuchenbecker KM, Nnadi CI, et al. Histone demethylase KDM5A is regulated by its reader domain through a positive-feedback mechanism. Nat Commun. 2015 Feb 17;6:6204. .

[44] Zhao D, Zhang Q, Liu Y, et al. H3K4me3 demethylase Kdm5a is required for NK cell activation by associating with p50 to suppress SOCS1. Cell Rep. 2016 Apr 12;15 (2):288–299.

[45] Wang C, Wang J, Li J, et al. KDM5A controls bone morphogenic protein 2-induced osteogenic differentiation of bone mesenchymal stem cells during osteoporosis. Cell Death Dis. 2016 Aug 11;7(8):e2335.